SCIREA Journal of Materials
http://www.scirea.org/journal/Materials
March 19, 2023
Volume 8, Issue 1, February 2023
https://doi.org/10.54647/materials430219

On the Melting of Metals

Hasse Fredriksson[*]
KTH (Royal Institute of Technology), Stockholm, Sweden
***Correspondence:** hassef@kth.se

Abstract

Thermal expansion is related to the atomic vibration amplitude. Owing to the anisotropy in the lattice, the amplitude will vary with the crystallographic direction, causing strain in the lattice. The strain caused by thermal expansion induces a force large enough to initiate plastic deformation of the metal at the beginning of melting. Deformation begins with the gliding of atoms along the gliding direction between two densely packed planes and corresponds to a certain atomic vibration amplitude in that specific direction. Two-dimensional clusters begin to form, and with the input of more energy, melting continues through the formation of three-dimensional clusters and lattice breakage. The heat of fusion corresponds to the energy required to rotate the clusters. When the lattice breaks down, strain energy in the solid is released. This causes a significant decrease in the binding energy between atoms in the liquid state compared to those in the solid state. The volume change during melting is related to changes in the binding energy between atoms in the solid and liquid states. The melting temperature is determined using this theory. The effects of stirring, pressure and gravity on the size of the clusters and melting point are discussed.

Keywords: cluster, heat capacity, heat of fusion, melting, metal, structure, temperature.

1. Introduction

Thermodynamics has often been used to analyse different types of phase transformations since the early days of Gibs. The field is based on strict mathematical relations in which experimental data are inserted to allow the analysis of transformations over a large range of variables. Thermodynamics is often used to analyse different solidification processes. The heating and melting of metals are less complex than the solidification process; however, there is no theory explaining the volume changes during melting nor the melting point.

Defining the melting point has been challenging for several years. In the late 19th century, Southerland (Southerland, 1890) presented a hard-sphere model of melting and discussed it as an effect of an increase in vibrational energy. Later, Lindemann (Lindemann, 1910) used the melting points of different species to discuss the amplitudes and frequencies of vibrations using Einstein's theory of heat capacity. Gilvarry (Gilvarry, 1956) used the Lindemann´s theory to determine the melting points of various species. The model states that when the amplitude of the vibrations exceeds a certain value, the bonds between atoms are broken. The value of the amplitude has been evaluated and is in the range of 10–20% of the atomic distances and it varies for different species. Gilvarry's analysis was later refined by Wallace (Wallace 1991) who obtained a good description of the melting points of several metals using this model.

Vibrations in the lattice cause strain. The effect of lattice strain on melting was discussed and analysed by Brillouin (Brillouin, 1938) and Born (Born, 1919); however, these lines of investigation were not followed up. Thermal expansion causes a strain in the lattice. This strain energy is stored in the material which was analysed by Gruneisen (Gruneisen, 1912), and is used to explain the difference between the heat capacity at constant volume, C_v, and at constant pressure, C_p.

Most metals are strongly anisotropic and exhibit different properties along different crystallographic directions. In particular, the shear modulus exhibits strong anisotropy. This anisotropy, along with thermal expansion, causes stress in the lattice. These stresses were analysed and related to the melting process. This analysis is based on the fact that the strain energy is a result of the difference in thermal expansion in different crystallographic directions. When the strain reached the plastic deformation threshold, melting of the species begin. The melting temperature and volume expansion during melting will be analysed. and determined theoretical. The heat of fusion and heat capacity of the liquid were analysed.

2. Thermal expansion

The thermal expansion and heat capacity of metals have been experimentally investigated. Figure 1a illustrates the heat capacity as a function of metal temperature. Figure 1b shows C_p of platinum up to its melting point. Figure 2 shows the principle of thermal expansion as a function of temperature. These figures show that the curves are identical at low temperatures and linear at temperatures above Debey's temperature. At temperatures lower than the Debey temperature, Gruneisen (Gruneisen, 1912) theoretically analysed the relationship between heat capacity and thermal expansion and derived a linear relationship between the two.

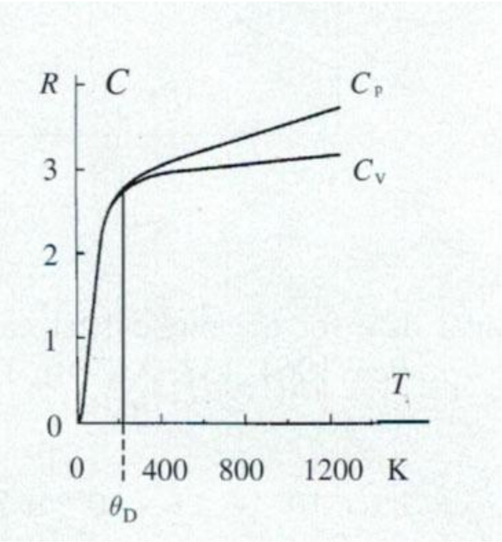

Figure 1a. Heat capacity as a function of temperature.

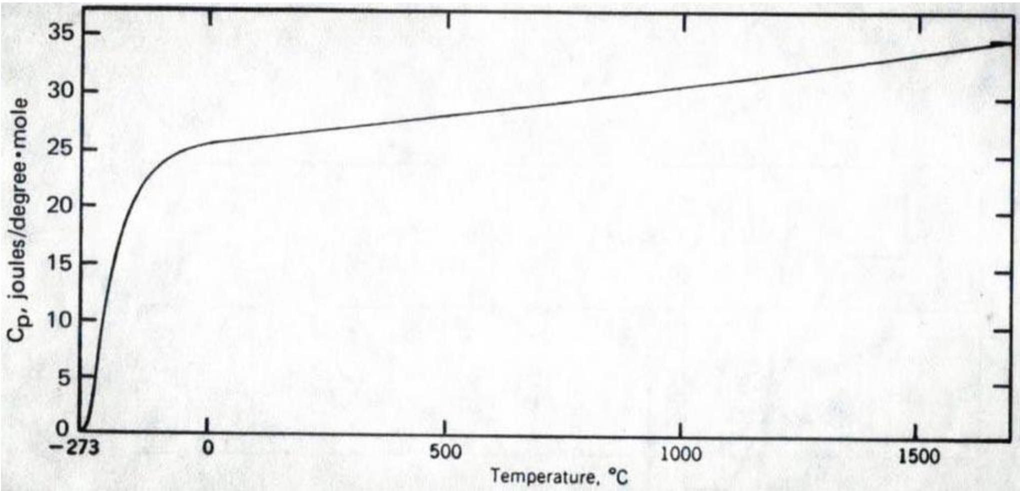

Figure 1b. Heat capacity as a function of temperature for platinum.

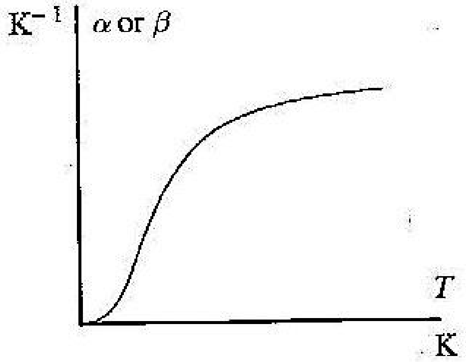

Figure 2. Thermal expansion as a function of temperature.

The expansion differed for different crystallographic directions and moduli. Such a difference should give rise to deformation of the unit cells in the species. However, X-ray analysis demonstrate that this is not the case. C_p, and C_v are equal below the Debye temperature, the effect of anisotropy on the expansion begins first at temperatures above the Debye temperature. Below this temperature, the atomic vibrations are not completely developed, and the longest wavelength are not in use. Expansion in the most important crystallographic directions and for cubic metals are expressed as follows:

$$\Delta\varepsilon_{100}^{BCC/FCC} = \alpha(T - \theta) \tag{1}$$

$$\Delta\varepsilon_{110}^{BCC/FCC} = 2^{\frac{1}{2}}\alpha(T - \theta) \tag{2}$$

$$\Delta\varepsilon_{111}^{BCC/FCC} = 3^{\frac{1}{2}}\alpha(T - \theta) \tag{3}$$

where:

$\Delta\varepsilon_{100}^{BCC/FCC}$= thermal expansion in Body centred-(BCC) or Face centred-metals (FCC) in the <100> direction.

$\Delta\varepsilon_{110}^{BCC}$= thermal expansion in BBC/FCC-metals in the <110> direction

$\Delta\varepsilon_{111}^{BCC/FCC}$ = thermal expansion in BBC/FCC-metals in the <111> direction

α = thermal expansion coefficient

T = temperature in Kelvin

θ = Debye temperature

3. Thermal strain and stress

Thermal expansion during heating accounts for a fraction of the work. Gryneisen used traditional thermodynamics to describe energy stored in a material. He described this using the following relation:

$$U_{Srain} = \frac{1}{2}\beta^2 V_m^{\theta}(T-\theta)^2 \mathrm{G} \qquad (4)$$

where:

U_{Srain} = thermal strain energy according to Gryneisen

β = volume expansion coefficient

V_m^{θ}= molar volume at the Debye temperature.

G = shear modulus

Gryneisen assumed that this energy describes the difference between C_p and C_v, and the relationship between them is expressed as follows:

$$C_p - C_v = \beta^2 V_m^{\theta}(T-\theta)G. \qquad (5)$$

The heat capacity can be easily determined experimentally, and the measured values can be used to compare the measured and calculated stored energy according to equation x. At the Debey temperature, C_p and C_v are both equal to 3R. From the Debey temperature to the melting point, the measurements demonstrated a linear increase in C_p, as shown in Figure 1b, whereas C_v is constant. The thermal energy, which is the difference between C_p and C_v, stored in the species from the Debey temperature to the melting point, can now be expressed as follows:

$$U_{Thermal} = (C_p^l - C_v)(T-\theta)^2 / 2(T_L-\theta) \qquad (6)$$

where:

$U_{Thermal}$ = thermal energy at heating related to the measured value of C_p

T= temperature, K

T_L= liquid temperature, K

C_v= heat capacity at the Debye temperature, J/mol

C_p^l= heat capacity at melting point, J/mol

This relationship is based on the fact that C_p increases linearly from the Debey temperature to the melting point (Figure 1b), which is assumed to be the case for most metals. According to the Gryneisens theoretical model, Equation 4 can be compared with the measured values described in equation 6. tables 2 and 3 summarize the energies at the melting points of some elements. The theory presented by Gryneisen provides a lower value of stored energy than that calculated from the heat capacity measurements. This is particularly true for elements with high stiffness. In the table, the calculations based on the shear modulus instead of the elastic modulus indicate that the strain energy calculated using the Gryneisens relation does not consider all the vibrations in the lattice, and it is most likely that the relations describe the transverse vibrations in the lattice. It is interesting to note that the values of the energy are close to the same at the melting point for most metals. The results listed in the table are used for determining volume changes during melting and for further analysis of the strain and stresses in the lattice.

TABLE 1. Physical constants.

Element	Structure	Volume thermal expansion 10^{-6}	Debey temperature K	Melting temperature K	Molar volume 10^{-6} m^3/mole
Na	BCC	70.6	158	371	23.69
K	BCC	83	91	337	45.3
Mo	BCC	4.98	450	2890	9.31
Al	FCC	23.1	428	934	9.99
Ni	FCC	12.7	450	1726	6.59
Cu	FCC	16.7	343	1356	7.09
Pd	FCC	11.6	274	1825	8.85
Pb	FCC	29	105	601	18.23

TABLE 2. Strain energies related to bulk and shear modulus.

Element	Bulk modulus 10^{10} N/M^2	Strain energy due to bulk modulus	Shear modulus 10^{10} N/M^2	Strain energy due to shear modulus
Na	6.9	1664		
K	3.2	2713		
Mo	33	2058	13	810
Al	7.36	452	2.6	159
Ni	19	1479	8	622
Cu	13.35	1220	4.6	420
Pd	18.44	2377	4.4	567
Pb	4.38	743	0.54	92
Mg				
Zn				
Zr				
Sb				
Si				

TABLE 3. Strain energy at the melting point, based on measurements of heat capacity.

Element	Heat Capacity at melting J/mol	Difference in Heat capacity C_p - C_v	Strain Energy Equation (4) J/mol
Na	31.93	6.99	1488
K	32.26	7.3	1796
Mo	52.35	27.30	66758
Al	33.69	8.75	4427
Ni	36.15	11.22	14316

Cu	33.31	8.37	8478
Pd	35.5	11.05	17138
Pb	30.7	5.9	2926
Mg	32.22	7.29	3785
Zn	29.55	4.66	2395
Zr	31.35	6.40	3329
Sb	30.93	5.90	3112
Si	28.29	3.37	1744

These relationships show that the strain energy is stored in the material during heating, resulting in changes in the potential energy. The Gryneisens relation does not consider the anisotropy of the material. As discussed previously, the expansion and modulus differ in different crystallographic directions, resulting in strain and stress in the lattice. However, owing to the symmetry of the lattice, a balance exists between these forces. The analysis will be concentrated on FCC and BCC metals.

The thermal expansion coefficient, α, describes the increase in the unit cell size. The thermal expansion was the lowest in the most densely packed direction. The thermal expansion is larger in all other directions. The expansion work varies in different directions. The smallest restriction of atom movements, which will start the melting process, will be in the Burgers vector's direction This analysis concentrated on determining the stress and strain difference between the densely packed directions and the two next densely packed directions. The difference was calculated from the Debey temperature up to the melting point and used to discuss the melting temperature.

For BCC metals, the most densely packed plane is {110}, and the most densely packed direction was <111>. This direction along with the <110> direction is analysed. The difference in the expansion between the nearest-neighbour atoms in this direction is as follows:

$$\Delta\varepsilon^{BCC}_{110/111} = \Delta\varepsilon^{BCC}_{110} - \Delta\varepsilon^{BCC}_{111} = (2^{\frac{1}{2}} - 3^{1/2}/2)\alpha(T - \theta) \qquad (7)$$

where:

$\Delta\varepsilon^{BCC}_{110/111}$ = length difference between the <110> and <111> direction in BCC lattice

The thermal strain from the Debey temperature to the melting point for different BCC metals was calculated for different elements using the above equations and is presented in Figure 4a. The data used in the calculations are listed in Table 4.

TABLE 4. Shear modulus, strain, and stress related to the lattice for BCC-metals

Element	Modulus in <100> direction 10^{10} N/m^2	Modulus in <110> direction	Modulus in <111> direction 10^{10} N/m^2	Stress 110/100 10^8	Strain 110/100
Na	0.59	0.07	0.24		0.082
K	0.26	0.045	0.115	1.1	0.0112
Mo	10.9	14.05	13	2.1	0.0067

This results in stress strains in this direction and compressive strains in the <111> direction. It would be interesting to calculate the change in stress in this crystallographic direction. The force or stress difference between two neighbouring atoms in the two directions is expressed as follows:

$$\Delta\sigma^{BCC}_{110/111} = (2^{\frac{1}{2}} G^{BCC}_{110} - 3^{1/2}/2 G^{BCC}_{111})\alpha(T - \theta) \qquad (8)$$

where:

$\Delta\sigma^{BCC}_{110/111}$ = stress difference in the most densely packed direction, <111>, the unit cell length, and the unit cell diagonal in BCC metals.

G^{BCC}_{110} = shear modulus in the <110> direction in BCC metals

G^{BCC}_{111} = shear modulus in the <111> direction for BCC metals

In Table 4, the stress and strain differences for the same BCC metals are summarized. Notably, the high stress inside the lattice is balanced by the lattice symmetry.

For the FCC metals the strain and the stress of interest, will be the <110> direction, which is the direction of Burgers vector. The largest effect on the strain in that direction will be given by the <100> direction all other directions have a much lower binding energy. The strain differences in these two directions are expressed as follows:

$$\mathit{\Delta}\varepsilon^{FCC}_{100/110} = \varepsilon^{FCC}_{100} - \varepsilon^{FCC}_{110} = (1 - 1/2^{1/2})\alpha(T - \theta) \tag{9}$$

where:

$\mathit{\Delta}\varepsilon^{FCC}_{100/110}$ = length difference between the <100> and <110> directions in FCC lattice

The stress difference is now given by the following relations for FCC metals

$$\mathit{\Delta}\sigma^{FCC}_{100/110} = (G^{FCC}_{100} - 1/2^{1/2}G^{FCC}_{110})\alpha(T - \theta) \tag{10}$$

where:

$\mathit{\Delta}\sigma^{FCC}_{110/100}$ = stress difference between the mostly densely packed direction, <110>, and the unit cell length for FCC metals.

G^{FCC}_{100} = shear modulus in the <100> direction for FCC metals

G^{FCC}_{110} = shear modulus in the <110> direction in FCC metals

Table 5 lists the strain and stress difference between the directions for some FCC metals. In addition, it is evident that the stress inside the lattice is a percentage of the modulus. Notably, the strains are almost equal for all the FCC metals

TABLE 5. Shear modulus, strain, and stress related to the lattice for FCC-metals

Element	Modulus in <100> direction 10^{10} N/m^2	Modulus in <110> direction	Modulus in <111> direction 10^{10} N/m^2	Stress 110/100 10^8	Strain 110/100
Al	2.82	2.30	2.48	1.4	0.0034
Ni	12.35	5.04	9.12	1.42	0.0047
Cu	7.54	2.35	4.08	0.74	0.0049
Pd	7.17	2.55	4.4	0.74	0.0053
Pb	1.49	0.36	0.54	1.	0.0042

4. Melting

The lattice vibrations differed in different crystallographic directions. The squared amplitude provides a relationship that describes kinetic energy. According to the equipartition relation, kinetic energy is equal to the potential energy given by the strain and stress in the lattice. The calculations listed in Table 5 demonstrate that the strain at melting points is almost equal for all FCC metals. For BCC metals, the strain is somewhat larger and has a larger difference; however, they are still very similar. The strain provided a certain value of the amplitude. It was concluded that the strain and amplitude reached certain values large enough to break the lattice.

Atoms, with an amplitude large enough in the direction with the smallest activation energy for flow, will start to move into other defects in the lattice. The plastic deformation of the lattice begins, the ordered atomic structure changes to a more unordered state, and the species start to melt. Most metals are plastically deformed by dislocations. Dislocations move along slip planes, where the activation energy of motion is very low. It is well known that in close-packed metals, the slip plane is the most densely packed {111} plane, and the slip direction for dislocations is along the <110> direction; for bcc, the slip plane is {110} and the slip direction is <111>. A previous study (Cottrell 1995) reported that the movement of dislocations starts at a stress range of 0.001–0.0001 of the elastic modulus. Near the melting point, all metals exhibited the same strain and energy values. These values were significantly large that they were expected to induce plastic deformation. The stress values listed in Table 4 also indicate that the stresses were large enough such that plastic flow began.

Thus, it can be concluded that melting occurred at a certain internal strain owing to the stress caused by thermal expansion. This strain corresponded to the amplitude in a certain direction. At a certain value of these amplitudes or a certain stress, the movement of the atoms begins, and two-dimensional (2D) clusters are formed inside the slip planes moving circularly. The same was true for the tensile tests of single crystals. Additional energy necessary for complete melting must be added to fully develop the clusters into three-dimensional (3D) clusters consisting of 10–11 atoms in the group. However, the internal energy induced by the thermal stress is released first. This energy corresponded to the energy related to the transverse wave energy in the lattice because liquids cannot undergo strain and they exhibit no transverse vibrations.

5. Volume expansion

It is well known that most liquid metals have larger volume than respective solids. During melting, the solid lattice was completely relaxed, and all the strains developed during thermal expansion were used to decrease the bonds between atoms. A new unordered cluster structure was formed, and additional energy was added to the system to rotate the clusters. The strain energy stored in the solid and released during the transformation was used to change the binding energy and increase the volume. The released strain energy is used in the work necessary to expand the volume. The following relationship is used to determine the expansion:

$$\Delta V = (\frac{U_{strain}}{G*V_m})^{1/2} \qquad (11)$$

where:

ΔV = volume difference between liquid and solid states.

Test calculations were performed for some elements and the results were compared with the measured values (Table 5). The strain energy values were obtained using the Gryneisen equation, and a reasonably good agreement was observed. The calculations were based on the bulk modulus of the solid. Part of the expansion occurred in a structure closer to the liquid, and a reduction in the bulk modulus by a factor of less than ten gives close-to-perfect agreement. The volume change corresponds to a change in the potential energy during melting. The kinetic energy is provided by the rotation of the clusters, and according to equipartition theories, is equal to the change in the potential energy or strain energy used for the volume expansion.

6. Heat capacity

The internal vibrational energies and heat capacities of solids are reasonably well understood, and the Einstein and Debye models are generally accepted theories that agree well with extensive experimental results. This situation is completely different from that of the heat capacity of liquids. The Einstein–Debye model is based on the anisotropy of the vibrations of atoms in the lattice. Because liquids are isotropic, atoms can vibrate freely in a liquid, and the temperatures reported by Einstein and Debye are significantly low. In contrast, solids exhibit fully developed vibrational energies above the Debye temperature. Here, it is assumed that the vibration energy is the same in the liquid and solid states at high temperatures and is abbreviated as 3R.

Neither strain energy nor energy from the transverse waves affected the energy of the liquid. The liquid consisted of clusters that rotate, and the total rotational energy was 3/2RT. As previously discussed. The clusters rotate continuously in the liquid and provide a heat capacity corresponding to 3/2R. Thus, it can be concluded that C_v is equal to (4 ½)R (3R; from vibrations and 3/2R; from rotations). Comparison of this with the measured values at the melting point showed reasonably good agreement, as summarized in Table 6.

TABLE 6. Heat capacity of liquid. Volume changes during melting.

Element	Heat Capacity of liquid J/mol	Fraction of Volume change on Melting Measured	Calculated Volume change Equation (11)
Na	31.81	0.025	0.03
Mo	34.23		0.025
Al	31.73	0.06	0.024
Ni	43.05	0.046	0.034
Cu	32.6	0.04	0.055
Pd			0,038
Pb	30.59	0.042	0.03

7. Discussion

Lindemann’s melting model is based on the fact that the lattice breaks down at a certain amplitude of vibration. This model is frequently used and has been thoroughly analysed theoretically by Wallace (Wallace, 1991).

The model presented in this study is based on Gruneisen’s theory, which states that vibrations build up strain in the lattice during heating. The strain energy is stored in the lattice and varies in different crystallographic directions. At a certain temperature, the strain supersedes the level of plastic flow. Plastic deformation begins in the direction where the activation energy for the flow is the least and the lattice is broken down. Deformations begin in the glide planes, and 2D clusters are formed. With the addition of heat, 3D clusters and cluster liquids were formed.

The general problem of determining the internal vibrational energies and heat capacities of liquids can be solved using the cluster model. A cluster is a permanent group of atoms held together by interatomic forces, which are weaker than the forces between atoms in crystals but are otherwise analogous. However, clusters do not exist permanently; they change over time, and the distance between atoms changes during vibrations. As discussed by Fredriksson (Fredriksson, 2005), this induces a rotational mechanism in the clusters. The increase in energy with temperature was described by one vibrational term and one rotational term, and the heat capacity was 41/2R (3R from the vibrations inside the clusters and 3/2R from the rotation of the clusters).

The lattice collapsed during melting, and the bonds between the atoms weakened. The stored strain energy was released and used to change the ordered solid state into a more unordered liquid state. The released strain energy corresponded to the volume change during melting.

Thermal analysis of the large metal samples showed differences between the heat capacities evaluated from the heating and cooling curves. This phenomenon can be explained as follows; during heating, the strain energy accumulates in the metal and is released during melting. During cooling from the melting point, no strain energy accumulates in the material. During heating, the experiments yielded the C_p , which denotes the value at a constant pressure. Cooling yielded the C_v, the heat capacity at a constant volume. This difference is given by Gruneisen’s law (Gruneisen, 1910).

Anisotropy in a solid lattice provides the forces for the internal strain necessary to melt a metal. However, several liquids transition to the amorphous state when cooled to a certain temperature. The amorphous phase was mostly formed by clusters in the melt. During cooling, the clusters were more stable and did not form crystals. Amorphous materials are typically subjected to strain. This was likely due to the formation of clusters with interacting atomic structures. This type of cluster formation might be very difficult for pure elements such as metals. This explains why no pure metals were observed to form amorphous structures directly in the liquid.

The melting point increased with pressure, following the classical thermodynamics described by the Clausius–Clapeyron law. Based on the model described above, it can be concluded that, with increasing pressure, the atoms come closer to each other, and it becomes more difficult for the atoms to start gliding between the densely packed planes. Pressure reduces the strain forces between the atomic directions in the lattice, making it more difficult for the atoms between the planes to rotate.

In the melting section, it was assumed that the atoms began to rotate during melting. Rotation was assumed to occur because of the atomic clusters. Clusters contain different fractions of atoms and their centre of mass is not necessarily at the spatial centre. Thus, gravity affects the relative movement of different clusters, and rotation decreases with decreasing gravity. Recently, a study on the effect of gravity on the heat of fusion and melting temperature was reported (Fredriksson, 2022). As previously discussed, an increase in the vibration amplitude resulted in the formation of larger clusters because of the decrease in the rotation rate with decreasing gravity. Note that the viscosity of a liquid is influenced by gravity.

8. Concluding remarks

The strain caused by thermal expansion during heating induces a force that causes gliding along the gliding direction between the two densely packed atomic planes. The strain corresponds to a certain amplitude of the atoms in a certain direction, and provides the possibility of moving in a direction where the activation energy for movement is sufficiently small. 2D rotation begins and, with increasing temperature, the lattice breaks down into clusters. The heavy point or electrically neutral point in the clusters was not equalised, creating a rotation of the clusters. The rotational energy corresponds to fusion heat. The volume change during melting was determined from the change in the binding energy of the liquid corresponding to the strain energy. This change causes volume expansion during melting.

References

[1] M. Born. (1919) Thermodynamics of Crystals and Melting. J. Chem. Phys: 243. 591–603.

[2] L. Brillouin (1938) On the thermal dependence of elasticity in Solids. Phys. Rev. 54,916–917.

[3] A. Cottrell. (1995) An introduction to Metallurgy, The Institute of Materials. 1995.

[4] J.J.Gilvarry. (1956) Phys.Review.102. 308.

[5] E. Gruneisen. (1912) Theorie des festen Zustndensenatomiger Elements, Annalen der Physik, 344257–306.

[6] H. Fredriksson, E. Fredriksson. (2005) A model of liquid metals and its relation to the solidification Process. Material Science & engineering. 413, 455–459.

[7] H. Fredriksson. (2022) Analysis of the Solidification Process of Metal Alloys Under Microgravity Conditions, Frontiers in Metals and Alloys

[8] F.A.Lindemann. (1910) Yber die Berechnung molekulaer Eigenfrequenzen. Physikalische Zeitschrift.11, (14), 609–614.

[9] W. Southerland. (1890) Phil. Mag. 30, 318

[10] D.C. Wallace. (1991) Mathematical and Physical Sciences. 433, 631–661.